Nanoscale

Accepted Manuscript

This article can be cited before page numbers have been issued, to do this please use: K. Katsiev, N. Lozova, L. Wang, S. Katla, R. Li, W. N. Mei, S. Skrabalak, C. Challa and Y. Losovyj, *Nanoscale*, 2016, DOI: 10.1039/C6NR02374F.

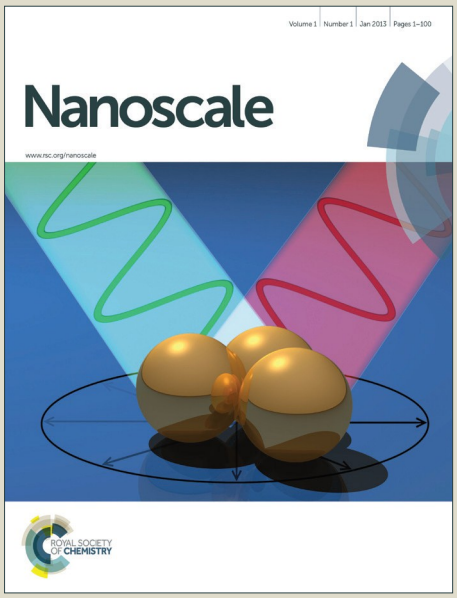

www.rsc.org/nanoscale

ROYAL SOCIETY OF CHEMISTRY View Article Online
DOI: 10.1039/C6NR02374F

Nanoscale

COMMUNICATION

Electronic Structure of Au_{25} Clusters: Between Discrete and Continuous

Received 00th January 20xx,
Accepted 00th January 20xx

DOI: 10.1039/x0xx00000x

www.rsc.org/

Khabiboulakh Katsiev[†], Nataliya Lozova[‡], Lu Wang[††], Katla Sai Krishna[‡], Ruipeng Li[‡‡], Wai-Ning Mei[††], Sara E. Skrabalak[§], Challa S. S. R. Kumar*[‡], and Yaroslav Losovyj*[§]

Here, an approach based on synchrotron resonant photoemission is employed to explore the transition between quantization and hybridization of the electronic structure in atomically precise ligand-stabilized nanoparticles. While the presence of ligands maintains quantization in Au_{25} clusters, their removal renders increased hybridization of the electronic states at the vicinity of the Fermi level. These observations are supported by DFT studies.

Ligand-stabilized metallic nanoparticles contain a metallic core with a continuous electronic conduction band in which the electrons move freely. However, quantization of the electron energy has been observed when nanoparticles become ultra-small (<2 nm in diameter).[1, 2] This transition is important as many of the physical and chemical properties – such as nature of energy spectra (continuous band to discrete), optical, crystal structure, chirality, magnetism, redox potential, femto-second dynamics and charge states of metallic nanoparticles – are altered when confined to this ultra-small size regime.[1] Unraveling the size-dependent physical, chemical, electronic and magnetic properties of ligand-stabilized metallic nanoparticles is of critical importance to understanding their catalytic properties.[3, 4] Although there are many studies on ultra-small metal nanoparticles,[2, 5, 6] to our knowledge, no investigations have studied the transition between the widely observed discrete (consisting of atomic and molecular orbital like states) and continuous or band like electronic structure (i.e. strongly hybridized states with band width). Here, synchrotron-based resonant photoemission spectroscopy (schematically represented in Fig. S1) and density functional theory (DFT) are combined to investigate this transition in the ligand-stabilized Au_{25} cluster $[Au_{25}(PPh_3)_{10}(SC_{12}H_{25})_5Cl_2]^{2+}$ (denoted herein as Au_{25}-*bi*) which is compared with $[Au_{25}(SCH_2CH_2Ph)_{18}]$ – (Au_{25}-*i*).

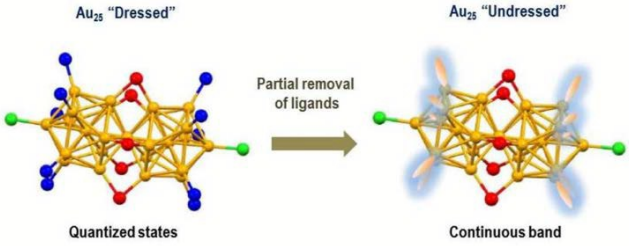

FIG.1 A schematic representation of transition from quantized states to hybridized band in [Au25(PPh3)10(SC12H25)5Cl2]$^{2+}$ – (Au25-bi) on partial removal of ligands (for simplicity only phosphine ligands shown removed). Yellow – Au, red – S, blue – P, green – Cl.

These Au_{25} clusters were selected because the phosphine ligands on Au_{25}-*bi* are easily removed under UHV conditions at room temperature, without aggregation or any major structural changes to the Au_{25} cores (based on experimental evidence as discussed below) to provide *in situ* generation of partially "undressed" gold cores and further comparison to the completely "dressed" Au_{25}-*i* clusters. Significantly, that "undressing" method is proven to be exclusively passive toward possible UHV assisted alteration (at least for the larger Au_{38} clusters[7]) - the only condition left under consideration in reported herein study which might influence the Au_{25} core.

The approach reported here is based on resonant photoemission enhancement from the 5*d* level of gold. Gold is a filled $5d^{10}$ system. Thus, resonant enhancement cannot be observed for atomic and molecular-like states due to the forbidden photoemission transition to a fully occupied 5*d* state at the $4f_{7/2}$ and $4f_{5/2}$ gold thresholds (Fig. S1). The resonant enhancement can only take place if 5*d* states hybridize with *s* and/or *p* state orbitals i.e. the atomic level broadens into hybridized band. This situation leads to a partial depletion of the *d*-band, permitting a photoemission resonant transition to a (*s(p)*-*d* hybridized) 5*d* state (Fig. S1). The core-hole

[§]*Department of Chemistry, Indiana University, Bloomington, Indiana 47405, United States, ylozovyy@indiana.edu*
[‡]*Center for Atomic-Level Catalyst Design, Cain Department of Chemical Engineering, Center for Advanced Microstructures and Devices (CAMD), Louisiana State University, Baton Rouge, Louisiana 70806, United State, ckumar1@lsu.edu*
[††]*Department of Physics, University of Nebraska at Omaha, Omaha, Nebraska 68182, United States*
[‡‡]*Cornell High Energy Synchrotron Source (CHESS), Cornell University, Ithaca, New York 14850, United States*
[†]*Department of Chemistry, Texas A&M University (TAMU), Texas 77843, United States, current address: King Abdullah University of Science and Technology (KAUST), Saudi Arabia*
Electronic Supplementary Information (ESI) available: Experimental details including chemicals, sample preparation, and characterization methods. Computation techniques, SV-AUC, GIWAXS, XPS, UPS, MALDI-TOF, ESI data of Au_{25} clusters. See DOI: 10.1039/x0xx00000x

decays through non-radiative Auger emission, enhancing direct photoemission but resulting in the same final state (see for details ESI, page 8). This resonance allows one to unambiguously determine if gold clusters still exhibit bulk metallic properties or have lost metallicity and instead exhibit molecular-like properties. $Au_{25}(SR)_{18}$ clusters were chosen for this case study as they are molecularly monodisperse and one of the smallest NCs with well-known structure, optical, chemo-physical properties, and established synthetic protocols.[8-13] X-ray crystallographic analysis of the $Au_{25}(SR)_{18}$ cluster revealed an icosahedral Au_{13} core, capped by an exterior shell composed of twelve Au atoms which are complexed with eighteen thiolate ligands.[11] Au_{25} clusters exhibit multiple molecular-like transitions in their optical absorption spectrum (see Fig. S2), with at least three well-defined bands at 1.8, 2.75, and 3.1 eV, consistent with literature report.[11] The study of its electronic structure by time-dependent DFT determined that the three lowest unoccupied MOs are mainly composed of 6*sp* hybrid atomic orbitals of gold, comprising the *sp* band, whereas the HOMO-1 through HOMO-5 are mainly weighted from the 5*d*[10] atomic orbitals of gold and thus constitute the *d*-band.[11] Single-crystal X-ray crystallographic analysis of *mixed* thiol/phosphine protected $Au_{25}(PPh_3)_{10}(SC_{12}H_{25})_5Cl_2$ (Au_{25}-*bi*) revealed that the core of the Au_{25} cluster is comprised of two vertex-shared Au_{13} icosahedra[14], i.e., a bi-icosahedron (see schematic on Fig.1). Recently the same group revealed a Au_{25} isomer, specifically that the cluster can include the same two vertex-shared icosahedra but rotated along a shared axis, forming the "twisted" rotamer.[15] The overall structure[14] can be described as four layers of Au pentagons having a staggered-eclipsed-staggered configuration, with ten PPh_3 ligands coordinated on top of peripheral Au atoms in layers one and four, five ethanethiolates bridging two of the Au_{25} pentagon rings in layers two and three, and two chlorides coordinating to two apical Au atoms.

In general, studies of the electronic structure of ligand-stabilized clusters exhibit a high level of complexity, wherein the *overall* electronic structure is strongly influenced by the Au core-ligand interaction.[16-20] Therefore, to gain insight into this ligand effect, we compared two Au_{25} clusters: the fully thiolated $Au_{25}(SCH_2CH_2Ph)_{18}$ (Au_{25}-*i*) cluster and the mixed thiol/phosphine $Au_{25}(PPh_3)_{10}(SC_{12}H_{25})_5Cl_2$ (Au_{25}-*bi*) cluster. Both clusters were synthesized using established synthetic protocols with slight modifications.[14, 21] Importantly, in the case of Au_{25}-*bi*, we found that ligand desorption could be facilitated simply in UHV, partially "undressing" the gold core and opening an avenue to study the surface of pristine, undressed clusters as well.

Sedimentation velocity-analytical ultracentrifugation (SV-AUC) [22] was used to confirm size uniformity, where the majority of species, ca 85%, are Au_{25} clusters (Fig. S3), assuring that the main contribution to the valence band photoemission signal is from Au_{25} species.

Photon energy dependent photoemission was employed to study the electronic structure of ligand-stabilized Au25-bi and Au25-i clusters. The photoemission spectra of both types of Au clusters deposited on the SiO_2 support were acquired at room temperature. The spectra acquired for the Au25-bi cluster revealed shallow 4f7/2 and 4f5/2 core levels, observed at 84.25 and 87.82 eV, respectively (Fig. 2a, Fig. S4); two valence band features are observed at about of 4.0 and 6.0 eV (Fig. 2b, Fig. S5). In general the electronic structure of thin films supported on various substrates is affected by

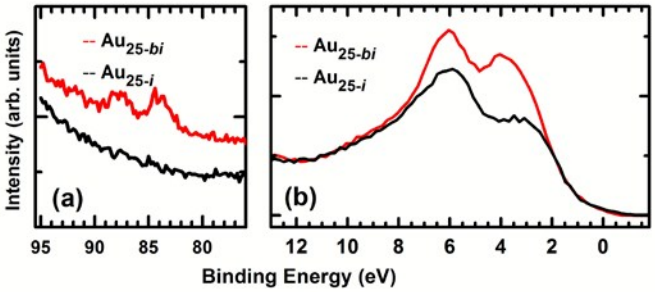

FIG.2 Core level (a) and valence band photoemission spectrum (b) of gold mixed-ligand bi-icosahedral-structure (Au25-bi) and thiol-stabilized icosahedral core-shell-structure (Au25-i) clusters drop casted on SiO2 native oxide surface of Si(111). Photon energy was (a)-120 eV and (b)-84 eV. Spectra were recorded at room temperature

film-substrate interaction. To exclude any influence from the substrate on the VB structure of the Au NC film, the films were made several hundreds of nanometers thick, i.e. three orders of magnitude thicker than the (ultra)thin film limit, at which the substrate might affect the interaction. Moreover the photon energy range that was used in the synchrotron photoemission experiments was selected to provide the highest surface sensitivity, limiting the sample probing depth to the topmost layers only. The XPS (which probes deeper layers compared to UPS) VB structures of the Au NC thick films deposited on various substrates looked virtually identical (Fig. S6), proving that the substrates were fully screened by Au cluster films.

Strongly enhanced photoemission at both the Au 4*f* core level and Au 5*d* valence band region observed for the Au_{25}-*bi* cluster compared to the Au_{25}-*i* cluster (Fig. 2, S5). This is due to enhanced phosphine (compared to thiol) ligand desorption from the gold clusters under the UHV conditions, which is consistent with much weaker Au-P, compared to Au-S, bonds.[23, 24] The desorption of weakly bound phosphine ligands results in freeing Au orbitals of Au_{25}-*bi* cluster and hence the observed photoemission enhancement. This enhancement clearly supports the role of ligand-controlled hybridization in determining the transition to continuous spectrum, as a significant portion of initially quantized gold valence band becomes delocalized when freed from gold-ligand bonding.

The stoichiometry of the Au cluster, investigated by X-ray core level photoemission (XPS), confirms a 1.4 Au/S ratio for the Au_{25}-*i* cluster (Fig. S11), as expected. In the case of the Au_{25}-*bi* cluster, measured ratios of Au/S=1 and Au/P=10 were obtained, indicating desorption of approximately 50% the thiol ligands and 80% of phosphine ligands, i.e. 11 out of 15 ligands have desorbed (Fig. 1, Fig. S10). That significant difference in ligand-to-core ratios remains after mild annealing (Fig. S4, Fig. S5) while demonstrating (similarly to room temperature) suppressed intensity of the valence band features as well as 4*f* gold core levels by thiol ligands (cluster Au_{25}-*i*) in comparison to Au_{25}-*bi* cluster cupped by mixed ligands. The chemistry of phosphines is dominated by their strong nucleophilicity and reducing character.[25] The presence of

View Article Online
DOI: 10.1039/C6NR02774B

nucleophilic phosphines in vicinity to the thiols weakens Au-S bounds in Au_{25}-*bi*, so about of half of thiol ligands desorb as well. The measured S $2p_{3/2}$ BE which is lower in Au_{25}-*bi* comparing to Au_{25}-*i* supports this picture (see Fig. S10, S11).

The great advantage of UHV-assisted ligand removal is the possibility to "undress" Au_{25}-*bi* clusters, allowing the electronic structure of the Au metal core to be probed *exclusively*, without any contribution from the ligand shell. This reduced level of complexity makes the study of the resonant photoemission enhancement from the gold valence band at the $4f_{7/2}$ and $4f_{5/2}$ threshold possible, which is indicative of an *f*-to-*d* transition. As mentioned, resonant enhancement of valence states in the photoemission spectra cannot be observed in *atomic* gold, as gold has fully occupied 5*d* orbitals. The photoemission resonance can only occur if *s*-*p*-*d* hybridization occurs, leading to partial depletion of the valence 5*d* bands in Au_{25}. Such resonant enhancement of the valence band photoemission was observed for Au_{25}-*bi* at photon energies corresponding to the gold $4f_{7/2}$ and $4f_{5/2}$ thresholds, indicative of an *f*-to-*d* transition (Fig. 3). The under-coordinated Au orbitals liberated upon ligand desorption, tend to

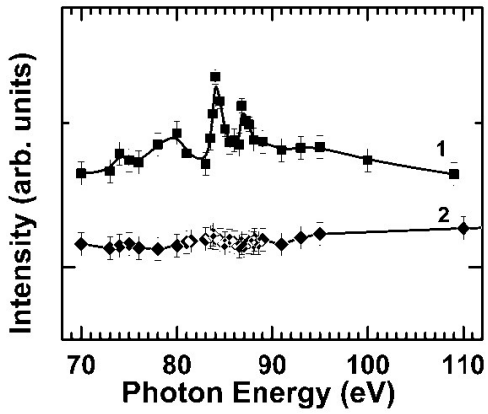

FIG.3. Photoemission intensities at binding energies of 3.5 eV versus photon energy, for gold mixed-ligand bi-icosahedral-structure Au_{25}-*bi* (1) and thiol-stabilized icosahedral Au_{25}-*i* clusters (2) deposited from solution on SiO_2 native oxide surface prepared on Si(111).

couple with each other partially depleting the valence 5*d* band and resulting in allowed *f*-*d* transitions. The photoemission studies of completely ligand free Cu, Ag and Au clusters[26, 27] reveal such hybridization effects through the formation of a continuous valence band for just 20 atoms per all clusters studied (the smallest 7 gold atoms cluster[27] was reported to exhibit either molecularlike or bulklike properties). Similarly, completely ligand free Au clusters very likely lose high symmetry geometry and demonstrate *s*-*d* hybridization.[28] The surface Au orbitals do not intercouple for Au_{25}-*i* because they are engaged in the core-thiolate ligand bonds. Thus, the resonance enhancement observed for Au_{25}-*bi* clusters is strongly suppressed for thiolate-protected Au_{25}-*i* clusters (Fig. 3, see for more detailed explanation SM, sections Ultraviolet Photoelectron Spectroscopy and Resonant Photoemission). This finding is in agreement with the superatom picture[29] extended by Häkkinen and co-workers to account for the closed electronic shell structure of gold-phosphine and gold-thiolate clusters.[30]

One might argue that the observed photoemission resonance originates from the larger size species comprised of agglomerated Au_{25}-*bi* clusters, caused by ligand desorption under vacuum in "undressing condition". To rule out this possibility, we performed grazing incident wide-angle X-ray scattering (GIWAXS) study that probes the sample's inter-particle distance on the macroscopic scale. The study revealed that the thin film formed by Au_{25}-*bi* clusters deposited onto the SiO_2, followed by UHV treatment, exhibits an ordered structure in the (001) orientation, with the (001) and (002) peaks along the q_z direction (Fig. S12). The interparticle spacing is 1.91nm from the (001) peak in GIWAXS pattern, whereas the nominal size of Au_{25} is 2.1 nm (including ligand shell).[22] The result confirms unaltered size of the Au_{25}-*bi* clusters and absence of any noticeable agglomeration after UHV treatment. Note, that for GIWAXS experiments we used the same sample that was previously characterized with XPS i.e. after the exposure to X-ray radiation under UHV. The cluster stability is also supported by observed *d*-band size trend and reduced DOS at the Fermi level (Fig. S7, S8), consistent with previously reported theoretical and experimental findings.[31-37]

DFT calculations were also conducted to probe the hybridization in gold and found to be consistent with the results from resonant photoemission. The DFT calculations were performed for a simple model, where the "undressed" Au_{25} cluster was adsorbed on SiO_2 (111) surface. The optimized structure of the Au_{25}:SiO_2 model is shown in Fig. S13. The Au_{25} cluster was found to be slightly positively charged. The projected density of states (PDOS) at the vicinity of the Fermi level (Fig. 4) reveals that electronic structure is intermixed with comparable density of 6*s* states, along with

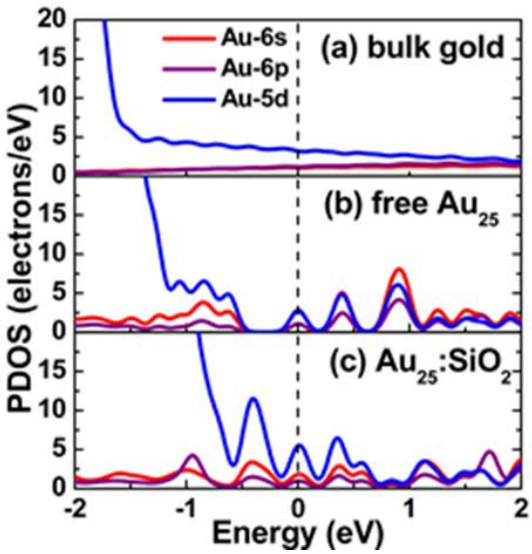

Figure 4. Projected 6*s*, 6*p*, and 5*d* density of states for Au atoms in (a) bulk gold, (b) gas phase free Au_{25} cluster, (c) Au_{25} adsorbed on SiO_2(111) surface. The dashed line indicates the Fermi level placement.

noticeable contributions from the Au 6*p* states. We also found clear overlaps between the occupied and unoccupied Au 6*s*, 6*p*, and 5*d* states in the vicinity of the Fermi level (Fig. 4) for bulk gold, the free Au_{25} cluster, and Au_{25}:SiO_2, suggesting the existence of *s*-*p*-*d* hybridization. PDOS away from Fermi region is dominated by Au 5*d* states (Fig. S14). It is worth noting that the substrate contribution to

the Au_{25} cluster electronic structure (one cluster thickness) deliberately was not excluded from our model, but even for such condition a significant mixing of gold 5*d* and 6*s* states at Fermi level along with notable density of 6p states emerges in calculation. This 6*p* and 6*s* somewhat weaker hybridization channel likely may supplement stronger *s-d* hybridization that facilitates the catalysis.

Conclusions

The synchrotron-based resonant photoemission spectroscopy revealed enhanced valence band photoemission that is much stronger at the 4*f* and weaker at the 5*p* core level Au thresholds (i.e. photoemission resonance enhancements) in partially "undressed" Au_{25}-*bi* clusters (a manifestation of *s-p-d* hybridization) while strongly suppressed in the "dressed" Au_{25}-*i* clusters. This observation unambiguously proves that noble metal clusters, even ultra-small size just of 25 gold atoms, still retain some bulk properties of gold. The DFT calculations that reveal overlap between these states in the vicinity of the Fermi level are in good agreement with the observed resonance, supporting partial depletion of the Au 5*d* states – a necessary condition for the photoemission resonance to occur. While the investigations reported here are the first attempts to study the influence of ligands in effecting the transition from hybridized band to discrete states in Au_{25} clusters, the methodology and the experimental techniques are broadly applicable to not only different sizes of Au clusters stabilized by various ligands but also to other types of metallic clusters. This approach is anticipated to pave new avenues for designing materials in correlation with their atomic or electronic constituents.

Acknowledgements

Research at the Center for Atomic-Level Catalyst Design (Energy Frontier Research Center) was funded by the U.S. Department of Energy, Office of Basic Energy Sciences under Award #DE-SC0001058. L. W and W.-N. M. acknowledge the support of Department of Energy (award #DE-EE0003174), Nebraska Center for Materials and Nanoscience, and the UNL Holland Computing Center with the associated USCMS Tier-2 site at the UNL. K.K acknowledge support of KAUST. Access to XPS is provided by NSF Award DMR MRI-1126394. The authors acknowledge helpful discussions with P. Dowben and O. Bakr.

References

1 H. Qian, M. Zhu, Z. Wu and R. Jin, Acc. Chem. Res., 2012, 45, 1470.
2 R. Jin and K. Nobusada, Nano Research, 2014, 7, 285-300.
3 M. L. Personick and C. A. Mirkin, J. Am. Chem. Soc., 2013, 135, 18238.
4 T. Takei, T. Akita, I. Nakamura, T. Fujitani, M. Okumura, K. Okazaki, J. Huang, T. Ishida and M. Haruta, in Advances in Catalysis, eds. C. G. Bruce and C. J. Friederike, Academic Press, 2012, vol. Volume 55, pp. 1-126.
5 T. Udayabhaskararao, M. S. Bootharaju and T. Pradeep, Nanoscale, 2013, 5, 9404.
6 X. Yuan, Z. Luo, Q. Zhang, X. Zhang, Y. Zheng, J. Y. Lee and J. Xie, ACS Nano, 2011, 5, 8800.
7 Y. B. Losovyj, S.-C. Li, N. Lozova, K. Katsiev, D. Stellwagen, U. Diebold, L. Kong and C. S. S. R. Kumar, J. Phys. Chem.y C, 2012, 116, 5857-5861.
8 Z. Wu, J. Chen and R. Jin, Adv. Funct. Mater., 2011, 21, 177
9 Y. Shichibu, Y. Negishi, T. Tsukuda and T. Teranishi, J. Am. Chem. Soc., 2005, 127, 13464.
10 G. H. Woehrle, M. G. Warner and J. E. Hutchison, The Journal of Physical Chemistry B, 2002, 106, 9979.
11 M. Zhu, C. M. Aikens, F. J. Hollander, G. C. Schatz and R. Jin, J. Am. Chem. Soc., 2008, 130, 5883.
12 Y. Negishi, N. K. Chaki, Y. Shichibu, R. L. Whetten and T. Tsukuda, J. Am. Chem. Soc., 2007, 129, 11322.
13 M. W. Heaven, A. Dass, P. S. White, K. M. Holt and R. W. Murray, J. Am. Chem. Soc., 2008, 130, 3754-3755.
14 Y. Shichibu, Y. Negishi, T. Watanabe, N. K. Chaki, H. Kawaguchi and T. Tsukuda, J. Phys. Chem..C, 2007, 111, 7845.
15 J.-i. Nishigaki, S. Yamazoe, S. Kohara, A. Fujiwara, W. Kurashige, Y. Negishi and T. Tsukuda, Chem. Commun., 2014, 50, 839.
16 O. Lopez-Acevedo, H. Tsunoyama, T. Tsukuda, H. Häkkinen and C. M. Aikens, J. Am. Chem. Soc., 2010, 132, 8210-8218.
17 F. Rissner, G. M. Rangger, O. T. Hofmann, A. M. Track, G. Heimel and E. Zojer, ACS Nano, 2009, 3, 3513-3520.
18 F. Rissner, D. A. Egger, L. Romaner, G. Heimel and E. Zojer, ACS Nano, 2010, 4, 6735.
1. N. Koch, A. Gerlach, S. Duhm, H. Glowatzki, G. Heimel, A. Vollmer, Y. Sakamoto, T. Suzuki, J. Zegenhagen, J. P. Rabe and F. Schreiber, J. Am. Chem. Soc., 2008, 130, 7300-7304.
20 G. Heimel, L. Romaner, E. Zojer and J.-L. Brédas, Nano Lett., 2007, 7, 932.
21 M. Zhu, E. Lanni, N. Garg, M. E. Bier and R. Jin, J. Am. Chem. Soc., 2008, 130, 1138-1139.
22 R. P. Carney, J. Y. Kim, H. Qian, R. Jin, H. Mehenni, F. Stellacci and O. M. Bakr, Nat Commun, 2011, 2, 335.
23 A. D. Jewell, E. C. H. Sykes and G. Kyriakou, ACS Nano, 2012, 6, 3545.
24 D. Krüger, H. Fuchs, R. Rousseau, D. Marx and M. Parrinello, J. Chem. Phys., 2001, 115, 4776.
25 J. A. Rodriguez, J. Dvorak, T. Jirsak, G. Liu, J. Hrbek, Y. Aray and C. González, J. Am. Chem. Soc., 2002, 125, 276.
26 K. J. Taylor, C. L. Pettiette-Hall, O. Cheshnovsky and R. E. Smalley, The Journal of Chemical Physics, 1992, 96, 3319.
27 J. Stanzel, M. Neeb, W. Eberhardt, P. G. Lisinetskaya, J. Petersen and R. Mitrić, Phys. Rev. A, 2012, 85, 013201.
28 H. Häkkinen, M. Moseler and U. Landman, Phys. Rev. Lett., 2002, 89, 033401.
29 R. B. Wyrwas, M. M. Alvarez, J. T. Khoury, R. C. Price, T. G. Schaaff and R. L. Whetten, The European Physical Journal D, 2007, 43, 91.
30 M. Walter, J. Akola, O. Lopez-Acevedo, P. D. Jadzinsky, G. Calero, C. J. Ackerson, R. L. Whetten, H. Grönbeck and H. Häkkinen, PNAS, 2008, 105, 9157.
31 B. Hammer and J. K. Nørskov, Surf. Sci., 1995, 343, 211-220.
32 G. Compagnini, A. A. Scalisi and O. Puglisi, Surf. Sci., 2006, 600, L1.
33 A. H. Larsen, J. Kleis, K. S. Thygesen, J. K. Nørskov and K. W. Jacobsen, Phys. Rev. B, 2011, 84, 245429.
34 B. Hammer, Y. Morikawa and J. K. Nørskov, Phys. Rev. Lett., 1996, 76, 2141.
35 A. Ruban, B. Hammer, P. Stoltze, H. L. Skriver and J. K. Nørskov, J. Mol. Catal. A: Chem., 1997, 115, 421.
36 A. Visikovskiy, H. Matsumoto, K. Mitsuhara, T. Nakada, T. Akita and Y. Kido, Phys. Rev. B, 2011, 83, 165428.
37 J. Liu, K. S. Krishna, Y. B. Losovyj, S. Chattopadhyay, N. Lozova, J. T. Miller, J. J. Spivey and C. S. S. R. Kumar, Chemistry – A European Journal, 2013, 19, 10201.